Closed-Form Models for Nonisothermal Effective Stress of Unsaturated Soils

Farshid Vahedifard, M.ASCE[1]; Toan Duc Cao, A.M.ASCE[2]; Ehsan Ghazanfari, M.ASCE[3]; and Sannith Kumar Thota, S.M.ASCE[4]

Abstract: Effective stress is a critical factor controlling the mechanical behavior of unsaturated soils. There has been an increasing interest toward fundamental and applied research on emerging applications that involve unsaturated soils subjected to elevated temperatures. However, major gaps remain in the development of a unified model that can properly represent temperature dependency of effective stress in unsaturated soils. The main objective of this study is to develop closed-form equations to describe the effective stress of unsaturated soils under nonisothermal conditions. For this purpose, suction stress-based formulations are developed for representing temperature-dependent suction stress and effective stress of unsaturated soils. The formulations incorporate temperature-dependent moist air pressure and matric suction into a skeleton stress equation originally developed using volume averaging. A nonisothermal soil water retention curve (SWRC) is used to account for thermal effects on the adsorbed water, surface tension, contact angle, and enthalpy of immersion per unit area. The validity of the model is examined by comparing predicted suction stress values against experimental data reported in the literature for various soils ranging from clay to sand. The effective stress equations developed in this study can provide further insight into the behavior of unsaturated soils under nonisothermal conditions. The models can be readily incorporated in numerical and analytical methods, leading to more accurate modeling of unsaturated soils subjected to nonisothermal loading conditions. **DOI: 10.1061/(ASCE)GT.1943-5606.0002094.**

Author keywords: Unsaturated soil; Effective stress; Nonisothermal condition; Thermo-hydro-mechanical coupling.

Introduction

Effective stress of unsaturated soils has posed a critical yet unsettled topic during the last few decades. The effective stress is recognized as the key factor controlling the engineering behavior of unsaturated soils including shear strength and volume change (e.g., Khalili et al. 2004; Lu and Likos 2004; Nuth and Laloui 2008). Since the pioneering work of Bishop (1959), several attempts have been made to study and properly model the effective stress of unsaturated soils from micro- to macroscales (e.g., Fredlund and Morgenstern 1977; Khalili and Khabbaz 1998; Li 2003; Khalili et al. 2005; Borja 2006; Lu and Likos 2006; Nuth and Laloui 2008; Alonso et al. 2010; Lu et al. 2010; Zhao et al. 2010; Nikooee et al. 2013; Manahiloh et al. 2016). Primarily built upon the average skeleton (or Bishop's) stress, the existing models commonly represent the effective stress of unsaturated soil as a function of all or a combination of matric suction, saturation level, and water retention properties of the soil (e.g., Wheeler et al. 2003; Sheng et al. 2004; Nuth and Laloui 2008; Lu et al. 2010). Supported by extensive experimental test results, the notion of effective stress has been employed for constitutive modeling of unsaturated soils under coupled processes (e.g., Jommi 2000; Loret and Khalili 2002; Sheng et al. 2004; Khalili et al. 2005; Gens et al. 2006; Mašín 2010). The latter implies that changes in effective stress fundamentally dominate the shear strength and volume change of unsaturated soils.

The effect of temperature on the effective stress of unsaturated soil is another important issue that certainly warrants further investigation (McCartney et al. 2019). There has been an increasing interest toward fundamental and applied research of the unsaturated soil behavior under elevated temperatures (e.g., Grant and Salehzadeh 1996; Cekerevac and Laloui 2004; Uchaipichat and Khalili 2009; Alsherif and McCartney 2015; Yavari et al. 2016; Zhou and Ng 2016; Ng et al. 2017). This growing interest is stimulated by the emergence of several nonisothermal applications such as earthen structure-atmosphere interaction under a changing climate, radioactive barriers, nuclear waste disposal, ground-source heat pumps for geothermal heating/cooling systems, buried high voltage cables, thermal energy storage systems, and thermally active earthen structures (e.g., Brandon et al. 1989; Laloui et al. 2006; Gens and Olivella 2001; Vahedifard et al. 2015; Alsherif and McCartney 2015; McCartney et al. 2016; Vahedifard et al. 2016; Robinson and Vahedifard 2016; Vahedifard et al. 2017). Some of the aforementioned applications can expose soil to elevated temperatures up to 100°C or even higher. Previous studies have demonstrated the promise in the use of the effective stress concept for describing the unsaturated soil behavior under elevated temperatures (e.g., Uchaipichat and Khalili 2009; Alsherif and McCartney 2015; Vega and McCartney 2015). This observation has led to the incorporation of effective stress into thermo-hydro-mechanical

[1]CEE Advisory Board Endowed Professor and Associate Professor, Dept. of Civil and Environmental Engineering, Mississippi State Univ., Mississippi State, MS 39762 (corresponding author). ORCID: https://orcid.org/0000-0001-8883-4533. Email: farshid@cee.msstate.edu

[2]Postdoctoral Associate, Center for Advanced Vehicular Systems and Dept. of Civil and Environmental Engineering, Mississippi State Univ., Mississippi State, MS 39762. Email: toand@cavs.msstate.edu

[3]Associate Professor, Dept. of Civil and Environmental Engineering, Univ. of Vermont, Burlington, VT 05405. Email: Ehsan.Ghazanfari@uvm.edu

[4]Graduate Student, Dept. of Civil and Environmental Engineering, Mississippi State Univ., Mississippi State, MS 39762. Email: st1545@msstate.edu

Note. This manuscript was submitted on February 26, 2018; approved on February 21, 2019; published online on July 9, 2019. Discussion period open until December 9, 2019; separate discussions must be submitted for individual papers. This paper is part of the ***Journal of Geotechnical and Geoenvironmental Engineering***, © ASCE, ISSN 1090-0241.

(THM) constitutive modeling of unsaturated soils (e.g., Thomas and He 1997; Loret and Khalili 2002; Laloui et al. 2003; Bolzon and Schrefler 2005; Laloui and Nuth 2009).

The use of effective stress in constitutive modeling of unsaturated soil offers several advantages including a smooth transition between saturated-unsaturated stages, the ability to incorporate hysteresis and hydraulic effects, and direct accounting of increase in strength (e.g., Sheng et al. 2004; Bolzon and Schrefler 2005). However, despite advances in THM constitutive models, major gaps still remain in the development of a unified effective stress that can properly describe all, or the majority of, aspects of the hydromechanical behavior of an unsaturated soil under elevated temperatures. Ideally, such model should be built upon the governing equations controlling the fully coupled THM behavior of unsaturated soil. Further, the effective stress model should consider the fact that the temperature can differently affect adsorption and capillarity (Fig. 1), two main water storage mechanisms in an unsaturated soil (e.g., Lu 2016; Vahedifard et al. 2018). Several studies have demonstrated the need for incorporating the capillary forces in the estimation of effective stress for saturated and unsaturated soils (e.g., Bishop 1959; Lambe and Whitman 1969; Mitchell 1976). Various parameters affect the magnitude of capillary forces in an unsaturated soil including the particle and pore size, pore water and pore air pressure, degree of saturation, surface tension, and soil-water contact angle (Lu and Likos 2006; Lu et al. 2010). Temperature is shown to affect the surface tension, contact angle of the soil-water interface, and enthalpy, which altogether can influence the water retention properties of an unsaturated soil (e.g., Villar and Gomez-Espina 2007; Vahedifard et al. 2018). Further, the adsorbed water, which relates to the residual saturation, is influenced by temperature (Revil and Lu 2013).

The main objective of this study is to develop closed-form equations to describe the effective stress of unsaturated soils under nonisothermal conditions. For this purpose, suction stress-based formulations are developed for representing effective stress of unsaturated soils subjected to varying temperature. The formulations incorporate temperature-dependent moist air pressure and matric suction into the effective stress expression presented by Lewis and Schrefler (1998). The effective stress equation is presented in a form comparable to Bishop's effective stress expression (Bishop 1959) but extended to nonisothermal conditions. The validity of the model is examined by comparing predicted suction stress values against experimental data reported in the literature for various soils ranging from clay to sand. The nonisothermal effective stress equations developed in this study can provide further insight into the behavior of unsaturated soils under thermal loading. The model can be also readily incorporated in numerical and analytical methods, leading to more accurate modeling of unsaturated soils subjected to nonisothermal loading conditions.

Underlying Theory and Formulations

The current study builds upon the nonisothermal effective stress expression presented by Lewis and Schrefler (1998), which was originally developed by Schrefler (1984) and Schrefler et al. (1990) using volume averaging. Employing this skeleton stress equation, we incorporate temperature-dependent moist air pressure and matric suction into a suction stress-based representation of effective stress. The latter is achieved by employing a nonisothermal soil water retention curve (SWRC) accounting for thermal effects on the adsorbed water, surface tension, contact angle, and enthalpy of immersion per unit area. This section provides a concise overview of the underlying theory of the effective stress expression presented by Lewis and Schrefler (1998). Interested readers are referred to Lewis and Schrefler (1998) for detailed discussion on the balance equations, upscaling approach, and thermodynamic constraints.

Following the work by Hassanizadeh and Gray (1979a, b) to apply thermodynamic constraints satisfying entropy inequality at the macroscopic level, Lewis and Schrefler (1998) used volume averaging based on the hybrid mixture theory to upscale balance equations from microscale to macroscale. The microscopic balance equations were integrated over a representative element volume (REV) (Fig. 1) to obtain the corresponding macroscopic balance equations. Lewis and Schrefler (1998) used four upscaled balance equations for mass (i.e., mass of solids, water, and moist air), linear momentum, angular momentum, and energy to derive the macroscopic mathematical formulations for a porous material subjected to THM processes. Appropriate constitutive equations were also employed to describe fluid and solid phases. In their formulations, the primary macroscopic variables include: moist air pressure (dry air pressure plus water vapor pressure) (u_a), capillary pressure (matric suction), temperature (T), and displacement. The capillary pressure is calculated as the difference between u_a and the pore water pressure (u_w) (i.e., $\psi = u_a - u_w$). Fig. 1 schematically shows an unsaturated soil consisting of three constituents (i.e., solids, water, air) at any temperature. Fig. 1(b) depicts a REV that is used to obtain averaged macroscopic quantities by integrating

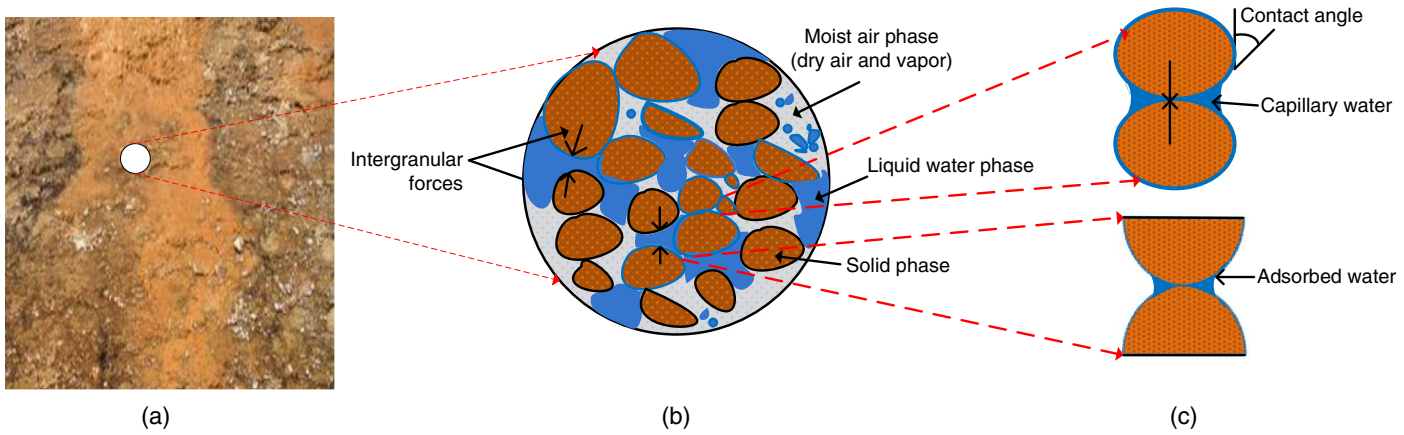

Fig. 1. Unsaturated soil consisting of three constituents at any temperature: (a) soil at macroscale; (b) representative element volume (REV); and (c) capillary and adsorbed water.

J. Geotech. Geoenviron. Eng., 2019, 145(9): 04019053

(averaging) a microscopic quantity through the averaging process. Lewis and Schrefler (1998) provide a detailed discussion about REV size requirements and boundaries between the micro- and macroscales. The averaging volume (i.e., REV) can be centered at each point in the system and must include all phases. The REV should be large enough so that averages are independent of the REV size and must be sufficiently small so that quantities such as gradients are meaningful at the macroscopic level.

Building upon the fully coupled THM formulation and following the work by Gray and Hassanizadeh (1991), Lewis and Schrefler (1998) showed that by implementing the balance laws in the entropy inequality and then imposing the required thermodynamic constraints into the conservation of linear momentum equation, one can obtain the following form for the nonisothermal effective stress of unsaturated soils:

$$\sigma' = \sigma - (S_w u_w + S_a u_a) \tag{1}$$

where σ' is the mean effective stress; σ is the total stress of mixture; and S_w and S_a are the degrees of saturation of water and moist air, respectively. Eq. (1) was originally developed by Schrefler (1984) and Schrefler et al. (1990) using volume averaging and is shown to be thermodynamically consistent (Gray and Schrefler 2001; Borja 2004). The equation was derived based on the assumption that the grains are incompressible, as opposed to skeleton (Lewis and Schrefler 1998). Eq. (1) can be rearranged in a form comparable to Bishop's effective stress expression (Bishop 1959) but extended to nonisothermal conditions

$$\sigma' = \sigma - u_a + \chi(u_a - u_w) \tag{2}$$

where χ is Bishop's effective stress parameter. While Bishop (1959) originally suggested to represent χ using S_w, more recent studies have shown that χ can be better represented by, e.g., Lu et al. (2010)

$$\chi \cong S_e \tag{3}$$

where S_e is the effective degree of saturation and can be obtained as

$$S_e = \frac{S_w - S_r}{1 - S_r} = \frac{\theta - \theta_r}{\theta_s - \theta_r} \tag{4}$$

where S_r is the degree of residual saturation; and θ, θ_s, and θ_r are the total, saturated, and residual water contents, respectively. Using S_e essentially implies that a portion of the water phase (i.e., residual water) is physically part of the solid phase because it is immobile.

As will be shown in the next sections, S_e (representing χ) and u_a can be linked to capillary pressure, adsorbed water, and temperature. Once these two parameters are obtained, one can use them along with Eq. (2) to determine the nonisothermal effective stress of unsaturated soil. The current study considers the effect of temperature on the pore space. Possible temperature effects on the solid phase such as the expansion of grains, and possible subsequent changes in the soil porous structure and solid configuration are not considered in the presented formulations.

Nonisothermal Residual Saturation

As suggested by Revil and Lu (2013), in this study the residual water content is considered to correspond to the adsorbed water. The nonisothermal residual water content can be addressed through quantifying the effect of temperature on adsorbed water (Vahedifard et al. 2018). By using a modified form of the Kelvin-Laplace equation, the adsorbed water can be expressed as (Revil and Lu 2013)

$$\theta_a = \theta_a^{\max}\left(\exp\left[-\frac{M_w\psi}{RT}\right]\right)^{1/M} \tag{5}$$

where $\theta_a^{\max}$ is the adsorption capacity; M is the adsorption strength; $M_w = 1.8 \times 10^{-5}$ m^3 mol^{-1} is the molar volume of water; and $R = 8.314$ J mol^{-1} K^{-1} is the universal gas constant. The adsorption strength, M, can be estimated to be equal to the shape fitting parameter of the van Genuchten (1980) model (Revil and Lu 2013). The nonisothermal residual saturation can be then defined as

$$S_r = \frac{\theta_a^{\max}}{\theta_s}\left(\exp\left[-\frac{M_w\psi}{RT}\right]\right)^{1/M} \tag{6}$$

The effective degree of saturation can be calculated as a function of S_w and S_r, as shown in Eq. (4), or obtained from the temperature-dependent capillary pressure as will be shown in the following section. The latter is used in the rest of this paper.

Nonisothermal Capillary Pressure

In this study, we use the nonisothermal SWRC formulations by Vahedifard et al. (2018), which consider the effects of temperature on adsorption and capillarity in unsaturated soils. The nonisothermal capillary pressure-saturation relationship accounts for the effect of temperature on surface tension, contact angle, and enthalpy of immersion per unit area.

As shown by Grant and Salehzadeh (1996), the temperature dependency of capillary pressure can be expressed as

$$\psi = \psi_{T_r}\left(\frac{\beta + T}{\beta_{T_r} + T_r}\right) \tag{7}$$

where ψ_{T_r} is the capillary pressure at the reference temperature T_r, β_{T_r} is the regression parameter at the reference temperature and the parameter β is calculated as (Grant and Salehzadeh 1996)

$$\beta = \frac{-\Delta h}{C_1} \tag{8}$$

where Δh is the enthalpy of immersion per unit area and C_1 is a constant, which can be determined as (Grant and Salehzadeh 1996)

$$C_1 = \frac{\Delta h_{T_r} + a(\cos\alpha)_{T_r} + b(\cos\alpha)_{T_r} T_r}{T_r} \tag{9}$$

where α is the temperature-dependent soil-water contact angle; and a and b are fitting parameters that can be estimated as (Haar et al. 1984; Dorsey 1940)

$$\begin{aligned} a &= 0.11766 \pm 0.00045\ Nm^{-1} \\ b &= -0.0001535 \pm 0.0000015\ Nm^{-1}K^{-1} \end{aligned} \tag{10}$$

A relationship between the enthalpy and temperature can be established by Watson (1943)

$$\Delta h = \Delta h_{T_r}\left(\frac{1 - T_r}{1 - T}\right)^{0.38} \tag{11}$$

where Δh_{T_r} is the enthalpy of immersion per unit area at the reference temperature. The temperature-dependent form of the contact angle can be obtained follows:

$$\cos\alpha = \frac{-\Delta h + TC_1}{a + bT} \tag{12}$$

Vahedifard et al. (2018) used the aforementioned equations for nonisothermal capillary pressure and adsorbed water to extend

three commonly used SWRC models originally developed by Brooks and Corey (1964) (referred to as BC), van Genuchten (1980) (referred to as VG), and Fredlund and Xing (1994) (referred to as FX) to nonisothermal conditions. Following Grant and Salehzadeh (1996), all nonisothermal SWRC formulations are written as a function of capillary pressure at the reference temperature. For this purpose, Eq. (7) is rearranged to solve for capillary pressure at the reference temperature and then is implemented into the SWRC formulations.

As shown by Vahedifard et al. (2018), the BC model can be extended to obtain the nonisothermal S_e, which represents the nonisothermal χ in the current study, as follows:

$$S_e = \left(\frac{p^b}{\psi\left(\frac{\beta_{T_r}+T_r}{\beta+T}\right)} \right)^{\lambda} \tag{13}$$

where p^b is the bubbling pressure in kPa; and λ is the pore size distribution index. Similar to the BC model, the nonisothermal extension of the VG model is written as follows:

$$S_e = \left(1 + \left(\alpha_{VG}\psi\left(\frac{\beta_{T_r}+T_r}{\beta+T}\right)\right)^{n_{VG}}\right)^{-m_{VG}} \tag{14}$$

where α_{VG} is a fitting parameter inversely related to the air-entry suction (1/kPa), n_{VG} is the pore-size distribution fitting parameter, and m_{VG} is a fitting parameter representing the overall geometry of the SWRC. In a similar manner, the nonisothermal FX model is expressed as follows (Vahedifard et al. 2018):

$$S_e = C(\psi)\left(\ln\left(e + \left(\frac{\psi\left(\frac{\beta_{T_r}+T_r}{\beta+T}\right)}{a_{FX}}\right)^{n_{FX}}\right)\right)^{-m_{FX}} \tag{15}$$

where $C(\psi)$ is a correction factor defined as

$$C(\psi) = \left(1 - \frac{\ln\left(1 + \frac{\psi\left(\frac{\beta_{T_r}+T_r}{\beta+T}\right)}{\psi_r}\right)}{\ln\left(1+\frac{\psi_{\max}}{\psi_r}\right)}\right) \tag{16}$$

where ψ_r is matric suction corresponding to the residual water content commonly set to be 1,500 kPa, $\psi_{\max}$ is the maximum matric suction corresponding to zero water content commonly set to be 10^6 kPa, n_{FX} is a fitting parameter related to pore size distribution, m_{FX} is a fitting parameter controlling the overall geometry of the SWRC, and a_{FX} is a fitting parameter related to the air-entry suction.

Nonisothermal Moist Air Pressure

To fully define the nonisothermal effective stress, one also needs to properly quantify the temperature effect on u_a. The moist air in the pore system is usually assumed to be a perfect mixture of two ideal gases, i.e., dry air and water vapor. The pressure and density (ρ_a) of the moist air can be considered as

$$u_a = u_{da} + u_{vap} \tag{17}$$

$$\rho_a = \rho_{da} + \rho_{vap} \tag{18}$$

where ρ_{da} and ρ_{vap} are the density of dry air and the vapor, respectively.

The two components contributing to the moist air pressure are linked to temperature as follows (Lewis and Schrefler 1998):

$$u_{da} = \rho_{da} TR/M_a \tag{19}$$

$$u_{vap} = \rho_{vap} TR/M_w \tag{20}$$

where $M_a = 0.028964$ kg mol^{-1} is the molar volume of dry air. In the current study, the dry air density is assumed to be temperature independent and is taken as 1.2041 kg/m^3. The saturated vapor density ρ_{vap} (kg/m^3) as a function of temperature can be expressed as (Saito et al. 2006)

$$\rho_{vap} = \frac{10^{-3} \times \exp\left(31.3716 - \frac{6014.79}{T} - 7.92495 \times 10^{-3} T\right)}{T} \tag{21}$$

By substituting Eqs. (19) and (20) into Eq. (17), the complete form of nonisothermal moist air pressure is defined as

$$u_a = \left(\frac{\rho_{da}}{M_a} + \frac{\rho_{vap}}{M_w}\right) TR \tag{22}$$

One can use the preceding equation to determine the effect of temperature on the net normal stress, $\sigma - u_a$. Fig. 2 depicts the temperature dependency of the water vapor pressure, dry air pressure, and moist air pressure for temperatures ranging from 10°C (283 K) to 100°C (373 K). The effect of temperature on the moist air pressure is significant, primarily due to an exponential increase in the water vapor pressure by temperature. The values shown in Fig. 2 represent the absolute values of moist air pressures. For calculating the effective stress, it is common to consider the moist air pressure compared to the atmospheric pressure (~101 kPa), leading to a zero value for the relative moist air pressure at the room temperature.

Closed-Form Solution for Nonisothermal Suction Stress and Effective Stress

The term $-\chi(u_a - u_w)$ in Bishop's effective stress expression is referred to as suction stress, σ^s (e.g., Karube et al. 1996; Lu and Likos 2004, 2006). Using this definition, Bishop's effective stress expression can be rewritten as

$$\sigma' = (\sigma - u_a) - \sigma^s \tag{23}$$

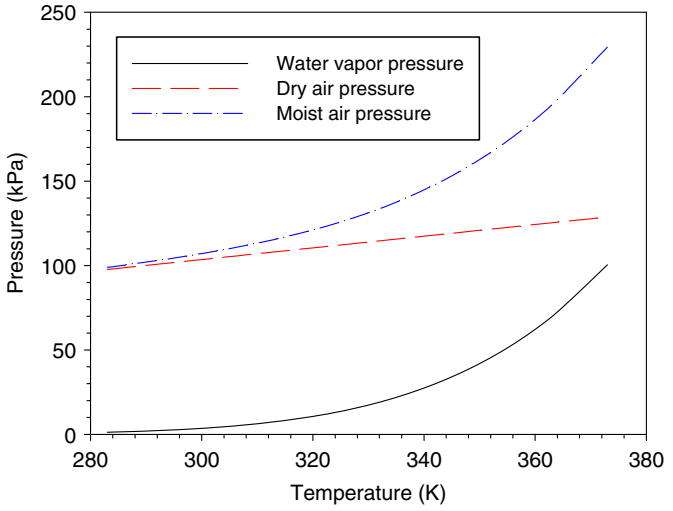

Fig. 2. Temperature dependency of water vapor pressure, dry air pressure, and moist air pressure.

where σ^s is the suction stress. Under ambient temperature, σ^s is defined as follows (Lu et al. 2010):

$$\sigma^s = -(S_e\psi)_{T_r} \tag{24}$$

The suction stress equation can be extended to nonisothermal conditions as

$$\sigma^s = -S_e\psi\left(\frac{\beta_{T_r}+T_r}{\beta+T}\right) \tag{25}$$

Alternatively, the nonisothermal suction stress can be obtained by extending the Khalili and Khabbaz (1998) model as follows:

$$\sigma^s = -\psi\left(\frac{\beta_{T_r}+T_r}{\beta+T}\right)\left(\frac{\psi\left(\frac{\beta_{T_r}+T_r}{\beta+T}\right)}{\psi_{aev}}\right)^{-\Omega_{KK}} \tag{26}$$

where ψ_{aev} is the bubbling pressure or the air entry suction; and Ω_{KK} the effective stress scaling parameter introduced by Khalili and Khabbaz (1998).

Depending upon the availability of fitting parameters, any of the extended SWRCs introduced in the previous sections can be used to define S_e in Eq. (24). The presented equations for nonisothermal suction stress and moist air pressure can be then substituted into Eq. (23) to develop complete expressions of nonisothermal effective stress. Using the BC model, the equations for nonisothermal suction stress and effective stress will be

$$\sigma^s = -\left(\frac{p^b}{\psi\left(\frac{\beta_{T_r}+T_r}{\beta+T}\right)}\right)^{\lambda}\psi\left(\frac{\beta_{T_r}+T_r}{\beta+T}\right) \tag{27}$$

$$\sigma' = \left(\sigma - \left(\frac{\rho_{da}}{M_a}+\frac{\rho_{vap}}{M_w}\right)TR\right) + \left(\frac{p^b}{\psi\left(\frac{\beta_{T_r}+T_r}{\beta+T}\right)}\right)^{\lambda}\psi\left(\frac{\beta_{T_r}+T_r}{\beta+T}\right) \tag{28}$$

Employing the VG model, we will have

$$\sigma^s = -\left(1+\left(\alpha_{VG}\psi\left(\frac{\beta_{T_r}+T_r}{\beta+T}\right)\right)^{n_{VG}}\right)^{-m_{VG}}\psi\left(\frac{\beta_{T_r}+T_r}{\beta+T}\right) \tag{29}$$

$$\sigma' = \left(\sigma - \left(\frac{\rho_{da}}{M_a}+\frac{\rho_{vap}}{M_w}\right)TR\right) + \left(1+\left(\alpha_{VG}\psi\left(\frac{\beta_{T_r}+T_r}{\beta+T}\right)\right)^{n_{VG}}\right)^{-m_{VG}}\psi\left(\frac{\beta_{T_r}+T_r}{\beta+T}\right) \tag{30}$$

For the FX model

$$\sigma^s = -\left(1-\frac{\ln\left(1+\frac{\psi\left(\frac{\beta_{T_r}+T_r}{\beta+T}\right)}{\psi_r}\right)}{\ln\left(1+\frac{\psi_{\max}}{\psi_r}\right)}\right) \times \left(\ln\left(e+\left(\frac{\psi\left(\frac{\beta_{T_r}+T_r}{\beta+T}\right)}{a_{FX}}\right)^{n_{FX}}\right)\right)^{-m_{FX}}\psi\left(\frac{\beta_{T_r}+T_r}{\beta+T}\right) \tag{31}$$

$$\sigma' = \left(\sigma - \left(\frac{\rho_{da}}{M_a}+\frac{\rho_{vap}}{M_w}\right)TR\right) + \left(1-\frac{\ln\left(1+\frac{\psi\left(\frac{\beta_{T_r}+T_r}{\beta+T}\right)}{\psi_r}\right)}{\ln\left(1+\frac{\psi_{\max}}{\psi_r}\right)}\right) \times \left(\ln\left(e+\left(\frac{\psi\left(\frac{\beta_{T_r}+T_r}{\beta+T}\right)}{a_{FX}}\right)^{n_{FX}}\right)\right)^{-m_{FX}}\psi\left(\frac{\beta_{T_r}+T_r}{\beta+T}\right) \tag{32}$$

Parametric Study

The proposed equations are employed to quantify the temperature effect on the effective degree of saturation, suction stress, and effective stress for Shonai dune sand, Pachapa loam, and Seochang sandy clay. Table 1 gives the parameters that are used for calculating the nonisothermal effective degree of saturation (using the extended VG model) and the suction stress for each soil. All the parameters except Δh_{T_r} values, which are reported for similar soils by Grant and Salehzadeh (1996), are obtained from Lu (2016). In all calculations, the moist air pressure compared to the atmospheric pressure is used, leading to zero air pressure at the room temperature.

Fig. 3 illustrates the effective degree of saturation and suction stress versus matric suction for Shonai dune sand, Pachapa loam, and Seochang sandy clay subjected to temperatures ranging from 25°C to 100°C. For Shonai dune sand, the matric suction varies between 0 and 8 kPa [Fig. 3(a)]. In such low matric suctions, capillarity is the dominant water storage mechanism and adsorption has minimal effect. It is seen that, for a given suction, higher temperature leads to lower S_e. For example, at the matric suction of 5 kPa, S_e decreases by approximately 13%, 39%, 49%, and 56% by increasing the temperature from 25°C to 40°C, 60°C, 80°C, and 100°C, respectively. This reduction can be attributed to changes in surface tension, contact angle, and enthalpy (Vahedifard et al. 2018). The results for Pachapa loam [Figs. 3(b and e)] and Seochang sandy clay [Figs. 3(c and f)] involve much higher suction values. However, the S_e sensitivity to temperature of Pachapa loam and Seochang sandy clay shows a similar trend to that presented for Shonai dune sand. For instance, the reduction of S_e for Pachapa loam [Fig. 3(b)] is approximately 14%, 24%, 33%, and 48% by increasing the temperature from 25°C to 40°C, 60°C, 80°C, and 100°C, at matric suction of 50 kPa. Further, the reduction of S_e for Seochang sandy clay [Fig. 3(c)] is approximately 10%, 17%, 23%, and 36% by increasing the temperature from 25°C to 40°C, 60°C, 80°C, and 100°C, at matric suction of 100 kPa. For Pachapa loam and Seochang sandy clay, the effect of temperature for suctions higher than 100 kPa becomes less significant.

The sensitivity of suction stress to temperature is shown in Figs. 3(d–f) for Shonai dune sand, Pachapa loam, and Seochang sandy clay, respectively. The trend of suction stress for all three soils is generally affected by temperature-induced changes in suction and effective degree of saturation. For Shonai dune sand [Fig. 3(d)], the suction stress exhibits a nonmonotonic behavior for each temperature. The absolute magnitude of suction stress first increases as matric suction increases. For each temperature, this increasing trend continues until reaching the air entry suction, which is about 0–2 kPa depending upon the temperature, [Fig. 3(a)]. Beyond the air entry suction in which the soil desaturates and transitions to the capillary zone, the absolute magnitude of suction stress decreases as long as the suction increases within the capillary zone. Once the soil reaches the residual saturation, suction stress increases by increases in matric suction. Applying higher temperatures leads to reduction in the air entry suction and the residual saturation. While in the saturated and capillary zones, increasing

Table 1. Input parameters for different soils used in parametric study

Soil	θ_s	θ_r	n_{VG}	Δh_{T_r} (J/m^2)	α_{VG} (1/kPa)	m_{VG}	T_r (K)
Shonai dune sand	0.43	0.03	5.565	−0.285	0.492	0.461	298
Pachapa loam	0.46	0.023	4.105	−0.516	0.111	0.144	
Seochang sandy clay	0.42	0.022	1.758	−0.516	0.117	0.228	

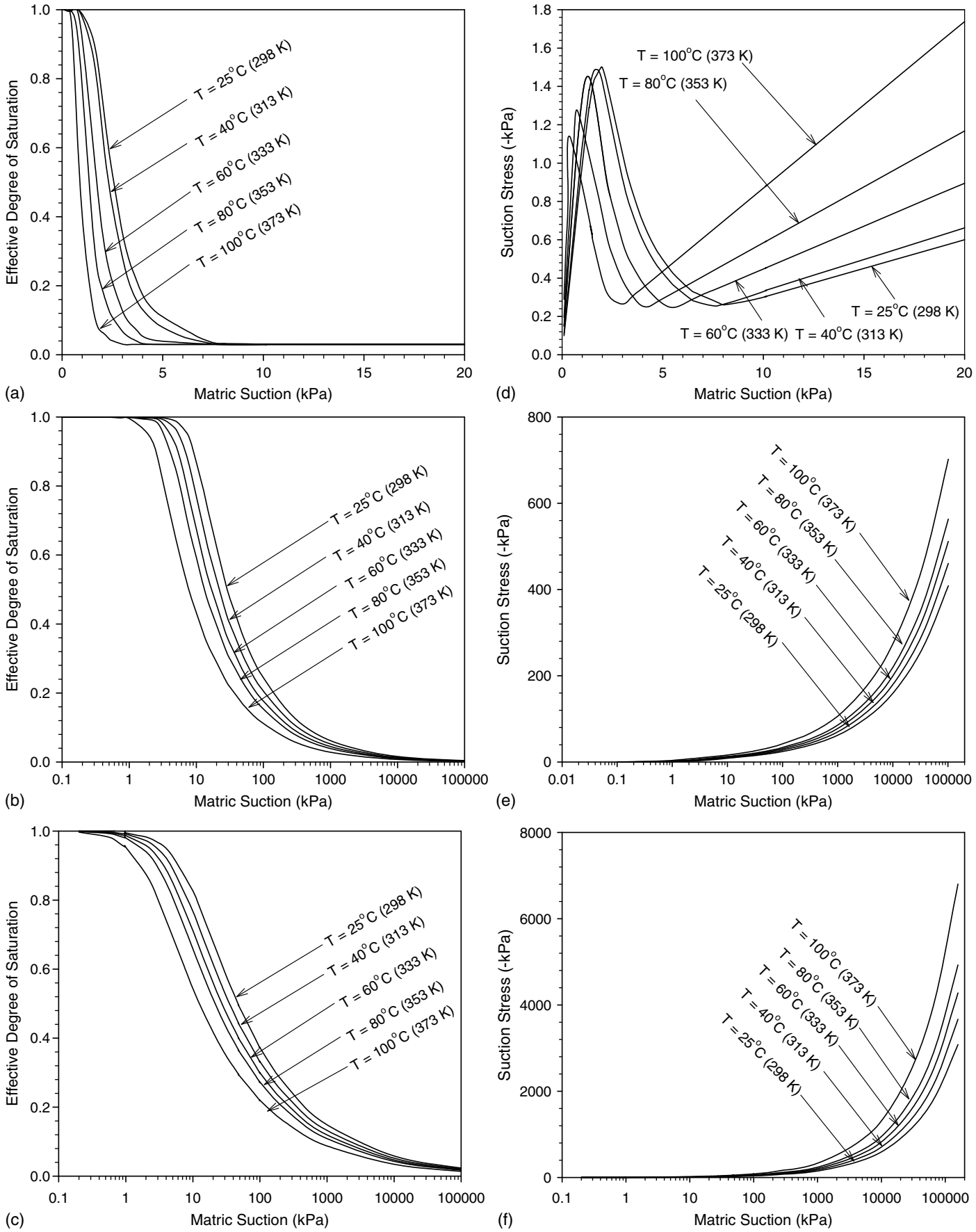

Fig. 3. (a–c) Effective degree of saturation and (d–f) suction stress versus matric suction for (a and d) Shonai dune sand; (b and e) Pachapa loam; and (c and f) Seochang sandy clay at different temperatures.

temperature leads to reduction in the absolute magnitude of suction stress at a given matric suction. After reaching the residual saturation, applying higher temperature increases absolute magnitude of suction stress at a given matric suction. The temperature effect in the saturated zone is consistent with the results reported by Campanella and Mitchell (1968) and Tanaka (1995). Unlike for Shonai dune sand, the suction stress versus matric suction at each temperature shows a monotonic trend for Pachapa loam [Fig. 3(e)] and Seochang sandy clay [Fig. 3(f)]. As expected, the ranges of matric suction and corresponding suction stress are much wider than that for Shonai dune sand. For Pachapa loam and Seochang sandy clay, the absolute suction stress gradually increases by increasing temperature from 25°C to 100°C because the effects of temperature on capillarity is more significant.

A main advantage of the proposed formulations is that the S_e equations only need material parameters at the reference temperature. That is, p^b and λ for the BC model, α_{VG}, n_{VG}, and m_{VG} for the VG model, and n_{FX}, m_{FX}, and a_{FX} for the FX model are only needed at the reference temperature. As clearly shown in Fig. 3, employing temperature-dependent contact angle and enthalpy of immersion addresses the effect of temperature on the air entry suction, which is shown to decrease as temperature increases.

To explicitly show the effect of temperature on effective stress, parametric studies are performed to determine nonisothermal effective stress at the total stress of 200 kPa, by accounting for the effect of temperature on the SWRC and moist air pressure. Fig. 4 illustrates the effective stress versus matric suction for Shonai dune sand subjected to temperatures ranging from 25°C to 100°C. At each temperature, the effective stress minimally increases by increasing matric suction. The latter is because, as shown previously, Shonai dune sand reaches the residual saturation in a low matric suction (~8 kPa), leading to a very small effective saturation throughout the range of matric suction examined. Fig. 4 includes an inset figure to better show the variation of effective stress at 25°C in low matric suction values (<5 kPa). The inset shows a nonmonotonic trend in this low suction range, stemming from the nonmonotonic suction stress trend for Shonai dune sand previously discussed in Fig. 3(d). A similar nonmonotonic trend is observed for the effective stress in low matric suction values at higher temperatures. As evident in Fig. 4, at a given matric suction, the effective stresses decrease by applying higher temperatures. This observation is consistent with the experimental results reported in the literature (e.g., Hueckel and Baldi 1990; Cekerevac and Laloui 2004; Alsherif and McCartney 2015) showing how the increase of temperature leads to reduction in the net normal stress as well as volumetric thermal expansion. At very high temperatures (e.g., 100°C) and low total stresses, the temperature-induced reduction of the effective stress may possibly lead to negative (tensile) effective stress.

Fig. 5 demonstrates the temperature dependency of effective stress for Pachapa loam at the given total stress of 200 kPa. For each temperature the effective stress increases as matric suction increases, with a rate that abruptly rises at high matric suction values. Applying higher temperatures is shown to decrease the effective stress up to the matric suction of approximately 20,000 kPa, which corresponds to the residual saturation. A similar trend is shown in Fig. 6 for Seochang sandy clay, where the residual saturation is reached at the matric suction of approximately 1,000 kPa. For these two soils, the temperature-induced reduction in effective stress up to the residual saturation can be attributed to temperature-induced changes in surface tension and contact angle, which in turn reduces the air entry value (Vahedifard et al. 2018). In this zone (i.e., capillarity region), the effects of temperature on effective degree of saturation and moist air pressure are significant. After reaching the residual saturation, the effects of temperature on capillarity becomes significant, thus the effective stress increases due to the increase of matric suction (while changes in effective degree of saturation are minimal). This observation suggests that heating the soil while the matric suction is in the residual region can lead to an increase in the effective stress, possibly explaining heat-induced hardening reported in the literature (e.g., Bolzon and Schrefler 2005; Cekerevac and Laloui 2004; Alsherif and McCartney 2015). It should be noted that the results beyond the residual suction should be interpreted

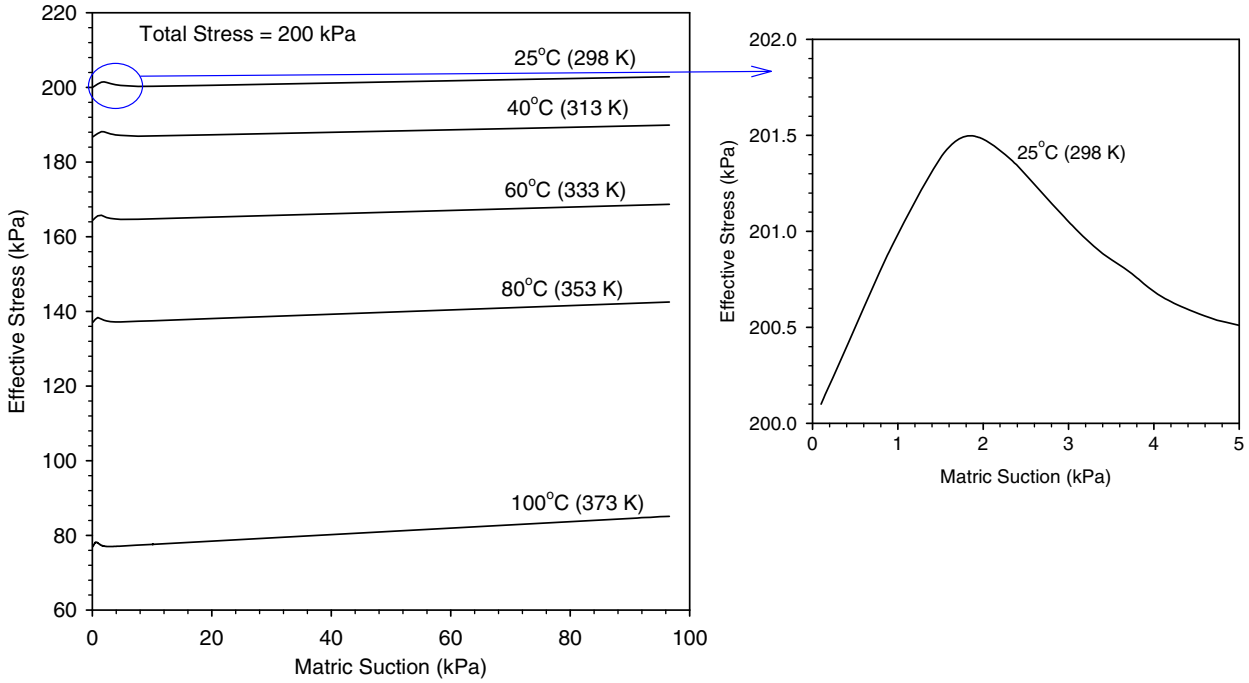

Fig. 4. Effective stress versus matric suction for Shonai dune sand at various temperatures, total stress = 200 kPa.

J. Geotech. Geoenviron. Eng., 2019, 145(9): 04019053

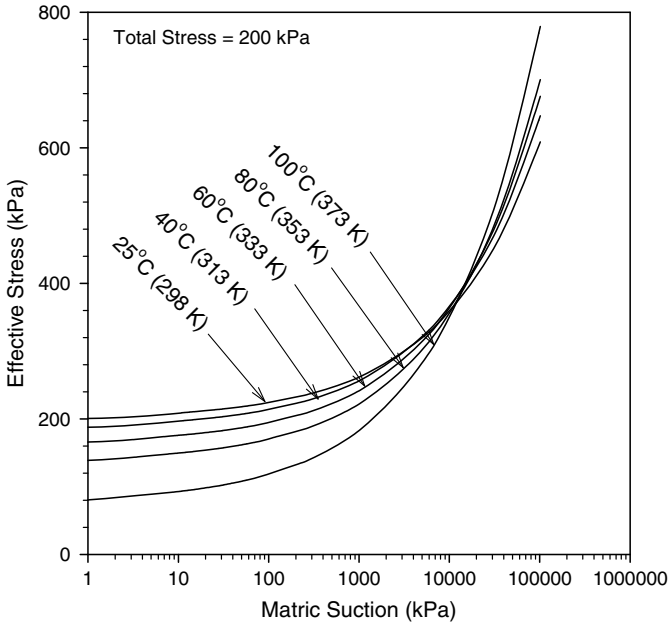

Fig. 5. Effective stress versus matric suction for Pachapa loam at various temperatures, total stress = 200 kPa.

with caution. Physically speaking, the phases become disconnected at the residual suction. At this time, imposing higher suctions at the boundary of sample may not necessarily lead to an equal increase in the suction inside the disconnected trapped phases due to incompressibility of the wetting phase. Thermodynamic-based formulations, such as that employed in this study, may not properly describe suction evolution for the disconnected phases. Further studies are certainly needed to provide insight into the variation of nonisothermal effective stress for suction levels higher than the residual suction.

Comparison against Experimental Data

Predicted values of nonisothermal effective degree of saturation and suction stress from the proposed formulations are compared against the results of experimental tests conducted on super-fine sand reported by Roshani and Sedano (2016), Bonny silt reported by Alsherif and McCartney (2014, 2015), and Gaomiaozi bentonite (GMZ01) reported by Ye et al. (2012). Further, the results are compared with those predicted by the Khalili and Khabbaz (1998) model [Eq. (26)]. Table 2 gives the fitting parameters used for calculating the nonisothermal effective degree of saturation and suction stress for the three soils that are examined. The SWRC parameters for each soil are taken from the original reference and the Δh_{T_r} values are adopted from the values reported by Grant and Salehzadeh (1996) for similar soils. The choice of the SWRC model for each soil is made based upon the model used in the original study.

Fig. 7 illustrates the predicted versus measured effective degree of saturation and suction stress for super-fine sand at temperatures of 20°C and 49°C. As shown in Figs. 7(a and b), the results from the proposed formulation are in close agreement with the measured effective degree of saturation values, with a root mean square error (RMSE) of 2.5 and 3.0. The predictive accuracy is higher than that from the SWRC model proposed by Roshani and Sedano (2016) (with RMSEs of 6.82 and 5.33). The SWRC model by Roshani and Sedano (2016) is an extended version of the FX model. The Roshani and Sedano (2016) SWRC model only accounts for the effect of temperature on the surface tension, leading to a lower accuracy than the model in the current study that considers the effects of temperature on the surface tension, the soil-water contact angle, and adsorption by the enthalpy of immersion per unit area (Vahedifard et al. 2018).

Figs. 7(c and d) compare the suction stress predicted from Eq. (31) with the experimental measurements by Roshani and Sedano (2016) and the predictions by the Khalili and Khabbaz (1998) model. The *measured suction stress* values shown in Figs. 7(c and d) are obtained by multiplying the measured matric

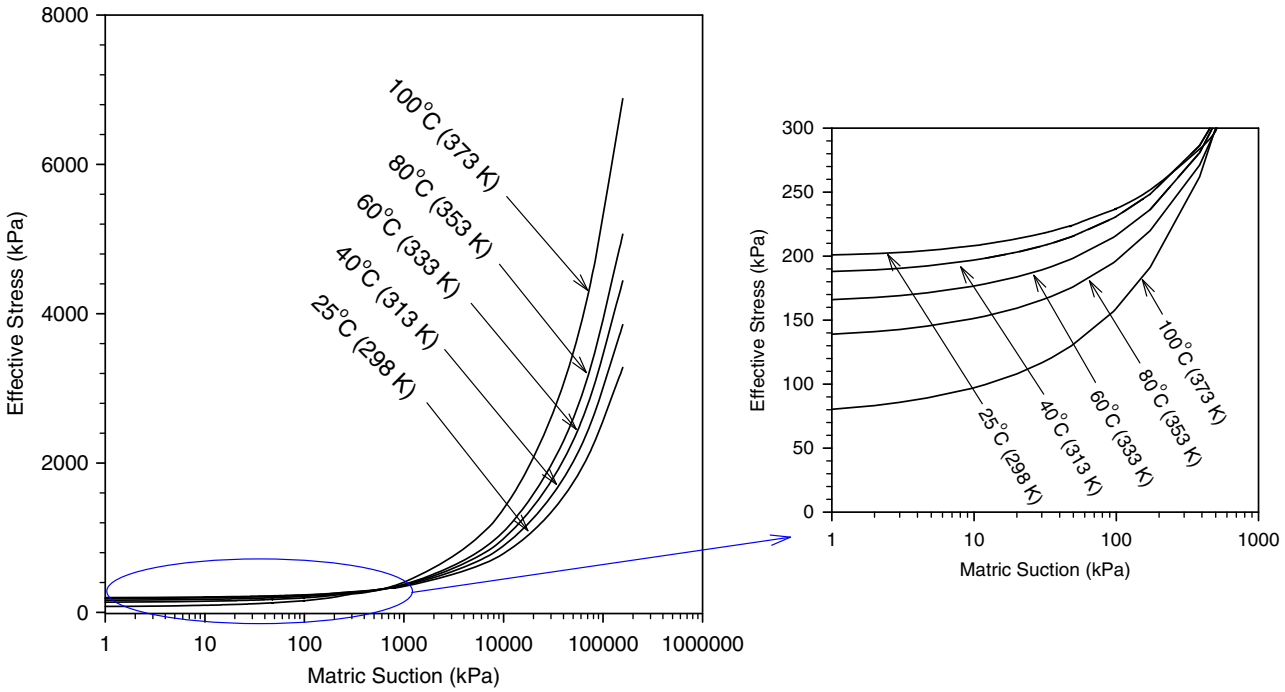

Fig. 6. Effective stress versus matric suction for Seochang sandy clay at various temperatures, total stress = 200 kPa.

Table 2. Parameters for calculating nonisothermal effective degree of saturation and suction stress

Soil	SWRC model	$\Delta h_{(T_r)}$ (J/m^2)	T_r (K)	SWRC parameters
Super-fine sand	FX	−0.285	293	$n_{FX} = 6.615$, $m_{FX} = 0.8488$, $a_{FX} = 4.6$ kPa, $\psi_r = 3.0$ MPa
Bonny silt	VG	−0.516	296	$n_{VG} = 1.61$, $m_{VG} = 0.3788$, $\alpha_{VG} = 0.33$ kPa^{-1}
GMZ01 bentonite	FX	−0.516	293	$n_{FX} = 0.8086$, $m_{FX} = 0.5864$, $a_{FX} = 8.0$ MPa, $\psi_r = 309$ MPa

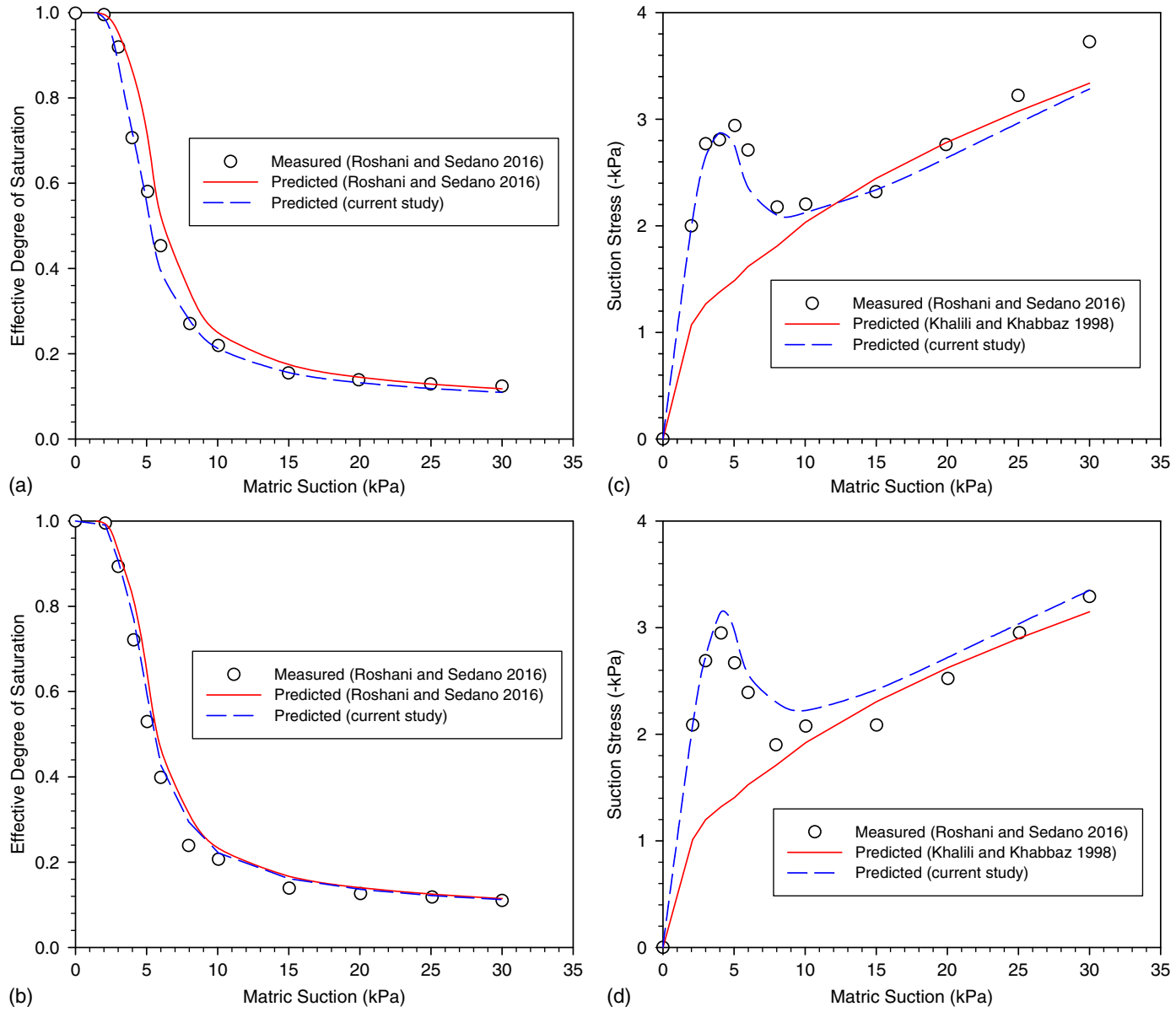

Fig. 7. Measured and predicted (a and b) effective degree of saturation; and (c and d) suction stress for super-fine sand at temperatures: (a and c) 20°C (293 K); and (b and d) 49°C (322 K).

suction by the measured effective saturation for each point as reported in the original reference. As shown, there is a very good agreement between the experimentally measured values and those attained from the proposed model (RMSE of 0.16 and 0.19). The proposed model yields a lower error than the Khalili and Khabbaz (1998) model (with RMSE of 0.85 and 0.92). In particular, the proposed model is able to capture the nonmonotonic trend of suction stress observed in the saturated and capillary zones for sandy soils, as discussed before for Fig. 3(d).

Figs. 8(a and b) depict the measured and predicted effective degree of saturation for Bonny silt at temperatures of 23°C [Fig. 8(a)] and 64°C [Fig. 8(b)]. The comparison reveals that the proposed model [Eq. (14)] can accurately replicate the experimental results. The effect of temperature on effective degree of saturation becomes insignificant at higher suction values that correspond to the residual region. Figs. 8(c and d) illustrate the measured and predicted suction stress values at temperatures 23°C and 64°C, respectively. Here also the data points obtained from the current model are closer to

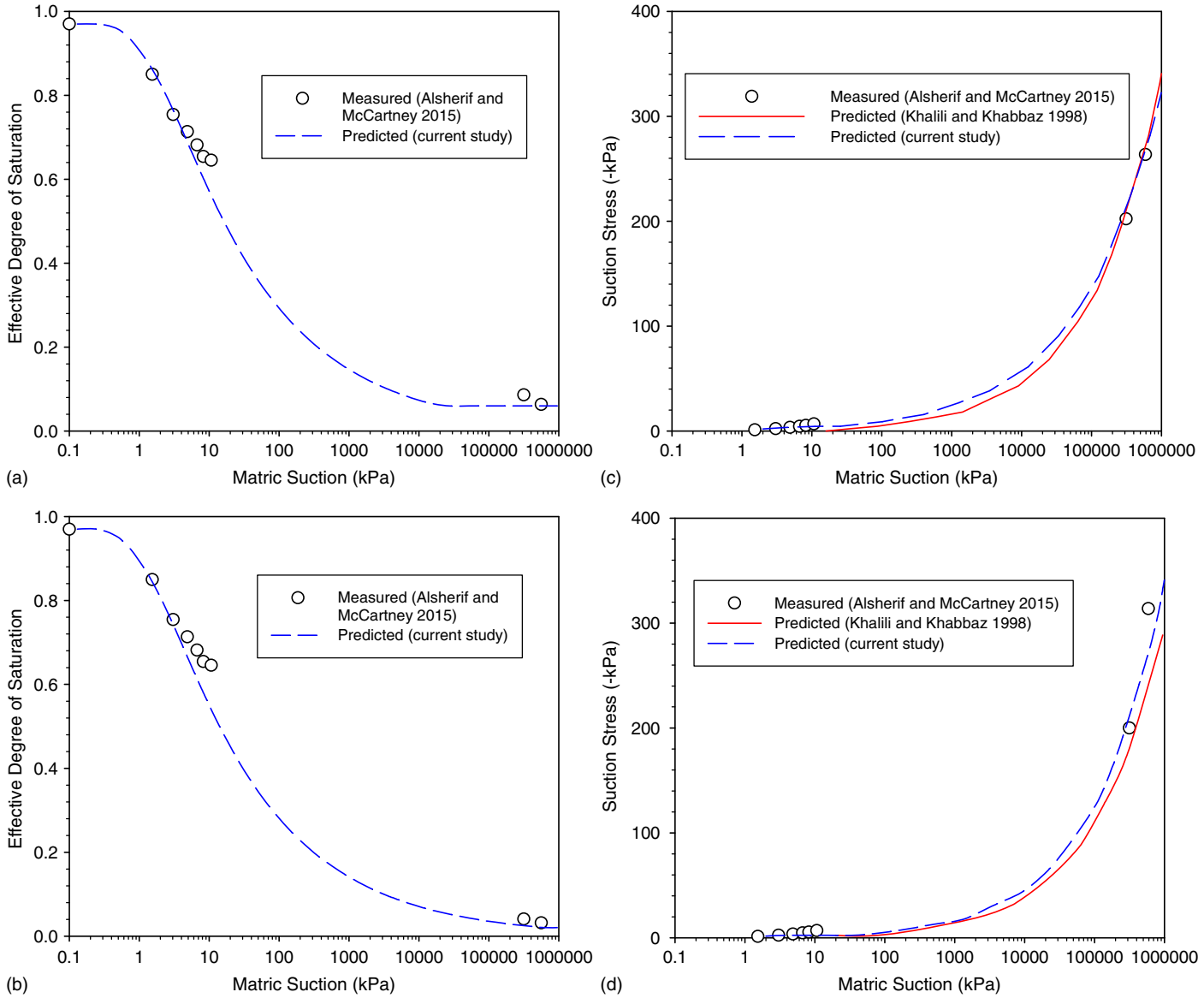

Fig. 8. Measured and predicted (a and b) effective degree of saturation; and (c and d) suction stress for Bonny silt at temperatures: (a and c) 23°C (296 K); and (b and d) 64°C (337 K).

the experimental data than those predicted by the Khalili and Khabbaz (1998) model. The effect of temperature on the suction stress at high matric suction values is more evident, which is due to the significant increase of matric suction while the effective degree of saturation remains almost constant in this region. It is noted that the experimentally measured points used to create Fig. 8 do not include data in the central portion of the retention curve, where the degree of saturation changes substantially. It would be desirable to have more test results in the central portion of the retention curve to gain a better understanding about the performance of the proposed formulations compared to other existing propositions.

Figs. 9(a and b) show a comparison between the experimentally measured effective degree of saturation data reported by Ye et al. (2012) and those predicted by the proposed model [Eq. (15)] for GMZ01 bentonite at temperatures 20°C and 60°C, respectively. The results show a very good match between the measured and predicted values (RMSEs of 1.1 and 0.9). Similarly, Figs. 9(c and d) suggest that the suction stress values from the proposed model [Eq. (29)] (RMSEs of 7.21 and 0.45) correspond very well with the measured points and better than from the Khalili and Khabbaz (1998) model (RMSEs of 11.74 and 3.27). The differences between the proposed nonisothermal suction stress and the Khalili and Khabbaz (1998) model can be explained as follows. The Khalili and Khabbaz (1998) model is a simple yet accurate model but it only uses one parameter (i.e., the effective stress scaling parameter) and a constant air entry suction. This allows this model to provide an accurate prediction for the suction stress at the ambient temperature. However, the proposed model in this study accounts for the effects of temperature on adsorption and capillary pressure as a function of contact angle, surface tension, and enthalpy. Another possible reason for the better performance of the proposed model compared to the Khalili and Khabbaz (1998) model can be due to the fact that the *measured suction stress points* for the proposed model in the current study are obtained based on the assumption that suction stress is equal to matric suction multiplied by the effective saturation. This assumption has been extensively tested and validated under isothermal conditions (e.g., Lu et al. 2010). Further studies are needed to examine the validity of this assumption for

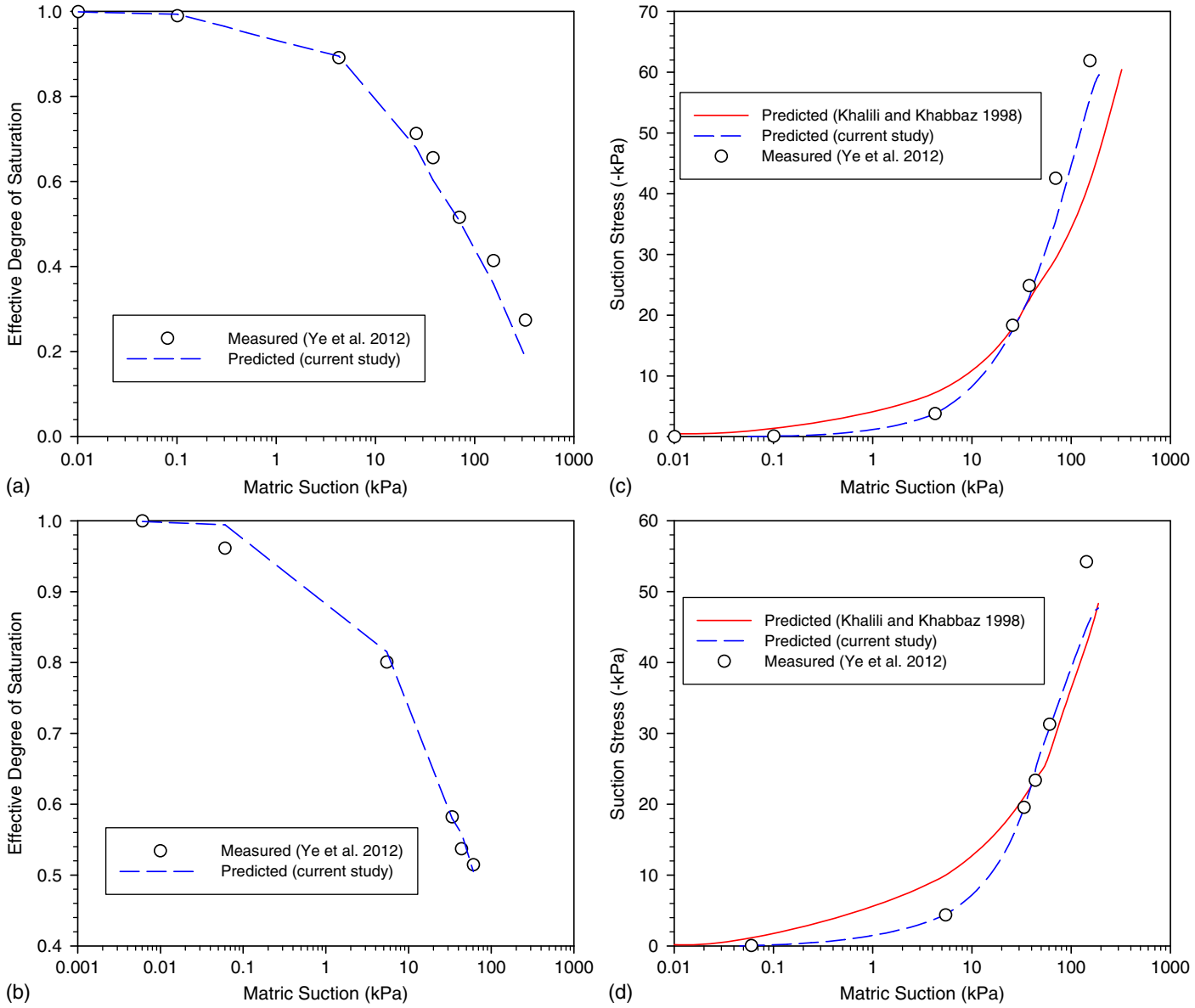

Fig. 9. Measured and predicted (a and b) effective degree of saturation; and (c and d) suction stress for GMZ01 bentonite at temperatures: (a and c) 20°C (293 K); and (b and d) 60°C (333 K).

nonisothermal conditions. For future studies, upon availability of appropriate experimental test results, it is suggested to back calculate suction stress values directly from temperature-controlled triaxial test results for a more thorough comparison of the proposed model against other equations of suction stress.

Conclusions

Considering the temperature dependency of effective stress can be an important step toward accurate modeling of the unsaturated soils behavior, particularly when dealing with applications that involve nonisothermal processes in unsaturated soils. The current study presented closed-form equations to describe the effective stress of unsaturated soil under nonisothermal conditions. The nonisothermal effective stress expressions are derived by considering the effects of temperature on adsorption, moist air pressure (i.e., dry air pressure plus water vapor pressure), and capillary pressure. The temperature dependency of capillary pressure involves the effects of temperature on the surface tension, the soil-water contact angle, and the enthalpy of immersion per unit area.

Employing the proposed formulations, parametric studies are performed to gain further insight into the effects of temperature on effective stress for three different soils. For Shonai dune sand, it is shown that elevated temperatures decrease the effective stress at a given matric suction. For Pachapa loam and Seochang sandy clay, applying higher temperatures is shown to decrease the effective stress up to the matric suction approximately corresponding to the residual saturation. Beyond this point, the effective stress increases by applying higher temperatures. In general, one can conclude that the effective stress trend versus temperature is heavily dominated by the temperature effect on the prevailing storage mechanism for each soil.

Predictions from the proposed formulations are compared and validated against experimental data available in the literature for sand, silt, and clay. The proposed closed-form equations for the nonisothermal effective stress can be considered to be a unified framework for describing flow and stress in unsaturated soils under

J. Geotech. Geoenviron. Eng., 2019, 145(9): 04019053

different temperatures. Findings of this study can be used to improve the modeling of the SWRC and effective stress in applications where meaningful temperature changes are expected in unsaturated soils such as those in emerging geotechnology applications.

Acknowledgments

This material is based upon work supported in part by the National Science Foundation under Grant No. CMMI-1634748. Any opinions, findings, and conclusions or recommendations expressed in this material are those of the authors and do not necessarily reflect the views of the National Science Foundation.

Notation

The following symbols are used in this paper:

a = fitting parameter for temperature-dependent surface tension;
a_{FX} = fitting parameter related to the air-entry suction in Fredlund and Xing's SWRC;
b = fitting parameter for temperature-dependent surface tension;
M = adsorption strength;
M_a = molar volume of dry air;
M_w = molar volume of water;
m_{FX} = Fredlund and Xing's fitting parameter controlling the overall geometry of the SWRC;
m_{VG} = van Genuchten's fitting parameter representing the overall geometry of the SWRC;
n_{FX} = Fredlund and Xing's fitting parameter related to pore size distribution;
n_{VG} = van Genuchten's pore-size distribution fitting parameter;
p^b = bubbling pressure in Brooks and Corey's SWRC;
R = universal gas constant;
S_a = degree of saturation of moist air;
S_e = effective degree of saturation;
S_r = degree of residual saturation;
S_w = degree of saturation of water;
T = absolute temperature;
T_r = reference temperature;
u_a = moist air pressure;
u_{da} = dry air pressure;
u_{vap} = water vapor pressure;
u_w = pore water pressure;
α = soil-water contact angle;
α_{VG} = van Genuchten's fitting parameter inversely related to the air-entry suction;
β = regression parameter used in temperature-dependent capillary pressure;
β_{T_r} = regression parameter at the reference temperature in temperature-dependent capillary pressure;
Δh = enthalpy of immersion per unit area;
Δh_{T_r} = enthalpy of immersion per unit area at the reference temperature;
χ = Bishop's effective stress parameter;
λ = pore size distribution index in Brooks and Corey's SWRC;
θ = total water content;
θ_a = adsorbed water content;
$\theta_a^{\max}$ = adsorption capacity;
θ_s = saturated water content;
θ_s = saturated water content;
θ_r = residual water content;
ρ_a = density of moist air;
ρ_{vap} = density of vapor;
ρ_{da} = density of dry air;
σ = total stress of mixture;
σ^s = suction stress;
σ' = effective stress;
ψ = matric suction (capillary pressure);
ψ_{aev} = bubbling pressure of Khalili and Khabbaz (1998) model;
ψ_{T_r} = capillary pressure at the reference temperature;
ψ_r = matric suction corresponding to the residual water content;
$\psi_{\max}$ = maximum matric suction corresponding to zero water content; and
Ω_{KK} = effective stress scaling parameter in the Khalili and Khabbaz (1998) model.

References

Alonso, E. E., J. M. Pereira, J. Vaunat, and S. Olivella. 2010. "A microstructurally based effective stress for unsaturated soils." *Géotechnique* 60 (12): 913–925. https://doi.org/10.1680/geot.8.P.002.

Alsherif, N. A., and J. S. McCartney. 2014. "Effective stress in unsaturated silt at low degrees of saturation." *Vadose Zone J.* 13 (5): 1–13. https://doi.org/10.2136/vzj2013.06.0109.

Alsherif, N. A., and J. S. McCartney. 2015. "Thermal behaviour of unsaturated silt at high suction magnitudes." *Geotechnique* 65 (9): 703–716. https://doi.org/10.1680/geot.14.P.049.

Bishop, A. W. 1959. "The principle of effective stress." *Teknisk ukeblad* 106 (39): 859–863.

Bolzon, G., and B. A. Schrefler. 2005. "Thermal effects in partially saturated soils: A constitutive model." *Int. J. Num. Anal. Methods Geomech.* 29 (9): 861–877. https://doi.org/10.1002/nag.437.

Borja, R. I. 2004. "Cam-clay plasticity. Part V: A mathematical framework for three-phase deformation and strain localization analyses of partially saturated porous media." *Comp. Meth. Appl. Mech. Eng.* 193 (48–51): 5301–5338. https://doi.org/10.1016/j.cma.2003.12.067.

Borja, R. I. 2006. "On the mechanical energy and effective stress in saturated and unsaturated porous continua." *Int. J. Solids Struct.* 43 (6): 1764–1786. https://doi.org/10.1016/j.ijsolstr.2005.04.045.

Brandon, T. L., J. K. Mitchell, and J. T. Cameron. 1989. "Thermal instability in buried cable backfills." *J. Geotech. Eng.* 115 (1): 38–55. https://doi.org/10.1061/(ASCE)0733-9410(1989)115:1(38).

Brooks, R. H., and A. T. Corey. 1964. *Hydraulic properties of porous media*. Fort Collins, CO: Colorado State Univ.

Campanella, R. G., and J. K. Mitchell. 1968. "Influence of temperature variations on soil behavior." *J. Soil Mech. Found. Div.* 94 (3): 709–734.

Cekerevac, C., and L. Laloui. 2004. "Experimental study of thermal effects on the mechanical behaviour of a clay." *Int. J. Num. Anal. Methods Geomech.* 28 (3): 209–228. https://doi.org/10.1002/nag.332.

Dorsey, N. E. 1940. *Properties of ordinary water substance*. New York: Reinhold.

Fredlund, D. G., and N. R. Morgenstern. 1977. "Stress state variables for unsaturated soils." *J. Geotech. Geoenviron. Eng.* 103 (5): 447–466.

Fredlund, D. G., and A. Xing. 1994. "Equations for the soil-water characteristic curve." *Can. Geotech. J.* 31 (4): 521–532. https://doi.org/10.1139/t94-061.

Gens, A., and S. Olivella. 2001. "Clay barriers in radioactive waste disposal." *Revue Française de Génie Civil* 5 (6): 845–856. https://doi.org/10.1080/12795119.2001.9692329.

Gens, A., M. Sánchez, and D. Sheng. 2006. "On constitutive modelling of unsaturated soils." *Acta Geotech.* 1 (3): 137–147. https://doi.org/10.1007/s11440-006-0013-9.

Grant, S. A., and A. Salehzadeh. 1996. "Calculation of temperature effects on wetting coefficients of porous solids and their capillary pressure functions." *Water Resour. Res.* 32 (2): 261–270. https://doi.org/10.1029/95WR02915.

Gray, W. G., and S. M. Hassanizadeh. 1991. "Unsaturated flow theory including interfacial phenomena." *Water Resour. Res.* 27 (8): 1855–1863. https://doi.org/10.1029/91WR01260.

Gray, W. G., and B. A. Schrefler. 2001. "Thermodynamic approach to effective stress in partially saturated porous media." *Eur. J. Mech. A/Solids* 20 (4): 521–538. https://doi.org/10.1016/S0997-7538(01)01158-5.

Haar, L., J. S. Gallagher, and G. S. Kell. 1984. *NBS/NRC steam table*. New York: Hemisphere Publ. Corp.

Hassanizadeh, M., and W. G. Gray. 1979a. "General conservation equations for multi-phase systems: 1. Averaging procedure." *Adv. Water Resour.* 2 (Mar): 131–144. https://doi.org/10.1016/0309-1708(79)90025-3.

Hassanizadeh, M., and W. G. Gray. 1979b. "General conservation equations for multi-phase systems: 2. Mass, momenta, energy, and entropy equations." *Adv. Water Resour.* 2 (4): 191–203. https://doi.org/10.1016/0309-1708(79)90035-6.

Hueckel, T., and G. Baldi. 1990. "Thermoplasticity of saturated clays: Experimental constitutive study." *J. Geotech. Eng.* 116 (12): 1778–1796. https://doi.org/10.1061/(ASCE)0733-9410(1990)116:12(1778).

Jommi, C. 2000. "Remarks on the constitutive modelling of unsaturated soils." In *Experimental evidence and theoretical approaches in unsaturated soils*, edited by A. Tarantino and C. Mancuso, 139–153. Rotterdam, Netherlands: A.A. Balkema.

Karube, D., S. Kato, K. Hamada, and M. Honda. 1996. "The relationship between the mechanical behavior and the state of pore water in unsaturated soil." [In Japanese.] *J. Jpn. Soc. Civ. Eng.* 535 (III-34): 83–92. https://doi.org/10.2208/jscej.1996.535_83.

Khalili, N., F. Geiser, and G. E. Blight. 2004. "Effective stress in unsaturated soils: Review with new evidence." *Int. J. Geomech.* 4 (2): 115–126. https://doi.org/10.1061/(ASCE)1532-3641(2004)4:2(115).

Khalili, N., and M. H. Khabbaz. 1998. "A unique relationship of chi for the determination of the shear strength of unsaturated soils." *Geotechnique* 48 (5): 681–687.https://doi.org/10.1680/geot.1998.48.5.681.

Khalili, N., R. Witt, L. Laloui, L. Vulliet, and A. Koliji. 2005. "Effective stress in double porous media with two immiscible fluids." *Geophys. Res. Lett.* 32 (15): L15309. https://doi.org/10.1029/2005GL023766.

Laloui, L., G. Klubertanz, and L. Vulliet. 2003. "Solid-liquid–air coupling in multiphase porous media." *Int. J. Num. Anal. Methods Geomech.* 27 (3): 183–206. https://doi.org/10.1002/nag.269.

Laloui, L., and M. Nuth. 2009. "On the use of the generalised effective stress in the constitutive modelling of unsaturated soils." *Comput. Geotech.* 36 (1): 20–23. https://doi.org/10.1016/j.compgeo.2008.03.002.

Laloui, L., M. Nuth, and L. Vulliet. 2006. "Experimental and numerical investigations of the behaviour of a heat exchanger pile." *Int. J. Num. Anal. Methods Geomech.* 30 (8): 763–781. https://doi.org/10.1002/nag.499.

Lambe, T. W., and R. V. Whitman. 1969. *Soil mechanics*, 553. New York: Wiley.

Lewis, R. W., and B. A. Schrefler. 1998. *The finite element method in the static and dynamic deformation and consolidation of porous media*. New York: Wiley.

Li, X. S. 2003. "Effective stress in unsaturated soil: A microstructural analysis." *Géotechnique* 53 (2): 273–277. https://doi.org/10.1680/geot.2003.53.2.273.

Loret, B., and N. Khalili. 2002. "An effective stress elastic-plastic model for unsaturated porous media." *Mech. Mater.* 34 (2): 97–116. https://doi.org/10.1016/S0167-6636(01)00092-8.

Lu, N. 2016. "Generalized soil water retention equation for adsorption and capillarity." *J. Geotech. Geoenviron. Eng.* 142 (10): 04016051. https://doi.org/10.1061/(ASCE)GT.1943-5606.0001524.

Lu, N., J. W. Godt, and D. T. Wu. 2010. "A closed-form equation for effective stress in unsaturated soils." *Water Resour. Res.* 46 (5): W05515. https://doi.org/10.1029/2009WR008646.

Lu, N., and W. J. Likos. 2004. *Unsaturated soil mechanics*. New York: Wiley.

Lu, N., and W. J. Likos. 2006. "Suction stress characteristic curve for unsaturated soil." *J. Geotech. Geoenviron. Eng.* 132 (2): 131–142. https://doi.org/10.1061/(ASCE)1090-0241(2006)132:2(131).

Manahiloh, K. N., B. Muhunthan, and W. J. Likos. 2016. "Microstructure-based effective stress formulation for unsaturated granular soils." *Int. J. Geomech.* 16 (6): D4016006. https://doi.org/10.1061/(ASCE)GM.1943-5622.0000617.

Mašín, D. 2010. "Predicting the dependency of a degree of saturation on void ratio and suction using effective stress principle for unsaturated soils." *Int. J. Num. Anal. Methods Geomech.* 34 (1): 73–90. https://doi.org/10.1002/nag.808.

McCartney, J. S., N. H. Jafari, T. Hueckel, M. Sánchez, and F. Vahedifard. 2016. "Emerging thermal issues in geotechnical engineering." In *Geotechnical fundamentals for addressing new world challenges: Springer series in geomechanics and geoengineering*, edited by N. Lu and J. Mitchell, 275–317. Cham, Switzerland: Springer. https://doi.org/10.1007/978-3-030-06249-1_10.

McCartney, J. S., M. Sánchez, and I. Tomac. 2016. "Energy geotechnics: Advances in subsurface energy recovery, storage, exchange, and waste management." *Comput. Geotech.* 75 (May): 244–256. https://doi.org/10.1016/j.compgeo.2016.01.002.

Mitchell, J. K. 1976. *Fundamentals of soil behavior*. New York: Wiley.

Ng, C. W. W., Q. Y. Mu, and C. Zhou. 2017. "Effects of soil structure on the shear behaviour of an unsaturated loess at different suctions and temperatures." *Can. Geotech. J.* 54 (2): 270–279. https://doi.org/10.1139/cgj-2016-0272.

Nikooee, E., G. Habibagahi, S. M. Hassanizadeh, and A. Ghahramani. 2013. "Effective stress in unsaturated soils: A thermodynamic approach based on the interfacial energy and hydromechanical coupling." *Transp. Porous Media* 96 (2): 369–396. https://doi.org/10.1007/s11242-012-0093-y.

Nuth, M., and L. Laloui. 2008. "Effective stress concept in unsaturated soils: Clarification and validation of a unified framework." *Int. J. Num. Anal. Methods Geomech.* 32 (7): 771–801. https://doi.org/10.1002/nag.645.

Revil, A., and N. Lu. 2013. "Unified water isotherms for clayey porous materials." *Water Resour. Res.* 49 (9): 5685–5699. https://doi.org/10.1002/wrcr.20426.

Robinson, J. D., and F. Vahedifard. 2016. "Weakening mechanisms imposed on California's levees under multiyear extreme drought." *Clim. Change* 137 (1): 1–14. https://doi.org/10.1007/s10584-016-1649-6.

Roshani, P., and J. A. I. Sedano. 2016. "Incorporating temperature effects in soil water characteristic curves." *Indian Geotech. J.* 46 (3): 309–318. https://doi.org/10.1007/s40098-016-0201-y.

Saito, H., J. Simunek, and B. P. Mohanty. 2006. "Numerical analysis of coupled water, vapor, and heat transport in the vadose zone." *Vadose Zone J.* 5 (2): 784–800. https://doi.org/10.2136/vzj2006.0007.

Schrefler, B. A. 1984. "The finite element method in soil consolidation (with applications to surface subsidence)." Ph.D. thesis, Dept. of Civil Engineering, Univ. College of Swansea.

Schrefler, B. A., L. Simoni, L. Xikui, and O. C. Zienkiewicz. 1990. "Mechanics of partially saturated porous media." In *Numerical methods and constitutive modelling in geomechanics*, edited by C. S. Desai and G. Gioda, 169–209. New York: Springer.

Sheng, D., S. W. Sloan, and A. Gens. 2004. "A constitutive model for unsaturated soils: Thermomechanical and computational aspects." *Comput. Mech.* 33 (6): 453–465. https://doi.org/10.1007/s00466-003-0545-x.

Tanaka, N. 1995. "Thermal elastic plastic behavior and modeling of saturated clays." Ph.D. thesis, Dept. of Civil and Geological Engineering, Univ. of Manitoba.

Thomas, H. R., and Y. He. 1997. "A coupled heat-moisture transfer theory for deformable unsaturated soil and its algorithmic implementation." *Int. J. Num. Methods Eng.* 40 (18): 3421–3441. https://doi.org/10.1002/(SICI)1097-0207(19970930)40:18<3421::AID-NME220>3.0.CO;2-C.

Uchaipichat, A., and N. Khalili. 2009. "Experimental investigation of thermo-hydro-mechanical behaviour of an unsaturated silt." *Géotechnique* 59 (4): 339–353. https://doi.org/10.1680/geot.2009.59.4.339.

Vahedifard, F., A. AghaKouchak, E. Ragno, S. Shahrokhabadi, and I. Mallakpour. 2017. "Lessons from the Oroville Dam." *Science* 355 (6330): 1139.2–1140. https://doi.org/10.1126/science.aan0171.

Vahedifard, F., A. AghaKouchak, and J. D. Robinson. 2015. "Drought threatens California's Levees." *Science* 349 (6250): 799. https://doi.org/10.1126/science.349.6250.799-a.

Vahedifard, F., T. D. Cao, S. K. Thota, and E. Ghazanfari. 2018. "Nonisothermal models for soil water retention curve." *J. Geotech. Geoenviron. Eng.* 144 (9): 04018061. https://doi.org/10.1061/(ASCE)GT.1943-5606.0001939.

Vahedifard, F., J. D. Robinson, and A. AghaKouchak. 2016. "Can protracted drought undermine the structural integrity of California's earthen levees?" *J. Geotech. Geoenviron. Eng.* 142 (6): 02516001. https://doi.org/10.1061/(ASCE)GT.1943-5606.0001465.

van Genuchten, M. T. 1980. "A closed-form equation for predicting the hydraulic conductivity of unsaturated soils." *Soil Sci. Soc. Am. J.* 44 (5): 892–898. https://doi.org/10.2136/sssaj1980.03615995004400050002x.

Vega, A., and J. S. McCartney. 2015. "Cyclic heating effects on thermal volume change of silt." *Environ. Geotech.* 2 (5): 257–268. https://doi.org/10.1680/envgeo.13.00022.

Villar, M. V., and R. Gomez-Espina. 2007. "Retention curves of two bentonites at high temperature." In Vol. 112 of *Proc., Experimental unsaturated soil mechanics*, edited by T. Schanz, 267–274. New York: Springer.

Watson, K. M. 1943. "Thermodynamics of the liquid state." *Ind. Eng. Chem.* 35 (4): 398–406. https://doi.org/10.1021/ie50400a004.

Wheeler, S. J., R. S. Sharma, and M. S. R. Buisson. 2003. "Coupling of hydraulic hysteresis and stress-strain behaviour in unsaturated soils." *Géotechnique* 53 (1): 41–54. https://doi.org/10.1680/geot.2003.53.1.41.

Yavari, N., A. M. Tang, J. M. Pereira, and G. Hassen. 2016. "Effect of temperature on the shear strength of soils and the soil-structure interface." *Can. Geotech. J.* 53 (7): 1186–1194. https://doi.org/10.1139/cgj-2015-0355.

Ye, W. M., Y. W. Zhang, B. Chen, Y. G. Chen, and Y. J. Cui. 2012. "Investigation on compressibility of highly compacted GMZ01 bentonite with suction and temperature control." *Nucl Eng Des.* 252 (Nov): 11–18. https://doi.org/10.1016/j.nucengdes.2012.06.037.

Zhao, C. G., Y. Liu, and F. P. Gao. 2010. "Work and energy equations and the principle of generalized effective stress for unsaturated soils." *Int. J. Num. Anal. Methods Geomech.* 34 (9): 920–936. https://doi.org/10.1002/nag.839.

Zhou, C., and C. W. W. Ng. 2016. "Effects of temperature and suction on plastic deformation of unsaturated silt under cyclic loads." *J. Mater. Civ. Eng.* 28 (12): 04016170. https://doi.org/10.1061/(ASCE)MT.1943-5533.0001685.